

## HIGHER HARMONIC VOLTAGES IN J-PARC RCS OPERATION

A. Schnase<sup>#</sup>, F. Tamura, M. Yamamoto, M. Nomura, K. Hasegawa, T. Shimada, H. Suzuki,  
JAEA/J-PARC, Tokai-mura, Ibaraki-ken, Japan 319-1195

C. Ohmori, M. Yoshii, E. Ezura, K. Hara, M. Toda, KEK, Tsukuba, Ibaraki-ken, Japan 305-0801.

### Abstract

The J-PARC Rapid Cycling Synchrotron (RCS) [1] uses broadband magnetic alloy loaded cavities to create the acceleration voltages needed for rapid cycling at 25 Hz rate. Besides the desired second harmonic of the acceleration frequency, which is employed in the painting process of RCS injection, also unwanted harmonics can be found at the acceleration gaps of the cavities. Here, the effect of the vector sums of undesired harmonics during the acceleration process is estimated.

### INTRODUCTION

In J-PARC, RCS MA-loaded cavities [2, 3] generate the acceleration voltages. The frequency range of the fundamental (h=2) as well as the 2<sup>nd</sup> harmonic (h=4) is covered in the same cavities without tuning loop. For this purpose, the Q-value of the RCS cavities filled with uncut cores with Q=0.5...0.7 is set to approximately Q=2 with an external inductor [4]. As example, Fig. 1 shows the impedance of cavity #5, one of the 11 cavities currently installed in RCS. Horizontal lines indicate the range of the harmonics 1-6, 8, 10.

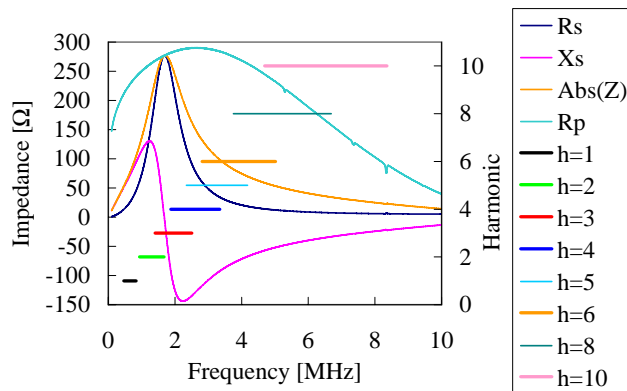


Figure 1: Impedance of cavity #5 (3 gaps in parallel).

The RCS beam interacts with the wideband cavities not only at the fundamental, but also at higher harmonics. The final stage amplifier in class AB with two tetrodes in push-pull mode is designed to cancel even harmonics, therefore (h=4) and (h=8) from amplifier are smaller than (h=6) and (h=10) respectively, as shown later in fig. 6.

An example of the harmonic content of the beam measured with a WCM (Wall Current Monitor) during an acceleration cycle with 2 bunches is shown in Fig. 2. The imbalance between both bunches is quite small, therefore the odd harmonics are negligible compared to the even harmonics. The small (h=3) peak near 5.5 ms is not related to the beam, because it appears without beam, too.

<sup>#</sup>Electronic mail address:  
Alexander.Schnase@J-PARC.JP

The relevant RCS parameters are shown in table 1. At 25 Hz operation and acceleration to 3 GeV the extracted beam power was approximately 20 kW.

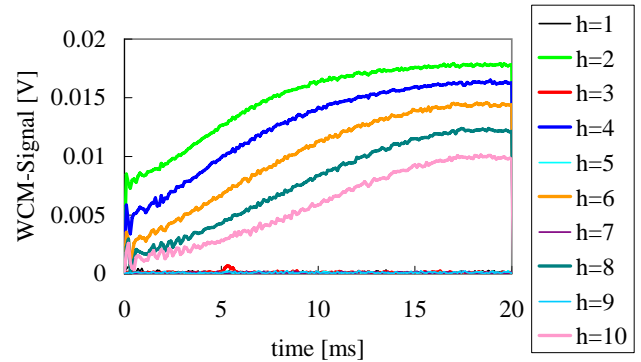


Figure 2: WCM harmonic content at 2-bunch RCS operation.

Table 1: RCS Machine injection conditions (2009/2/17)

Injection Energy	181 MeV
Revolution frequency	469.0875 kHz
Fundamental frequency (h=2)	938.175 kHz
Sum of RCS cavity voltages	76 kV
Peak current from Linac	5mA (2 RCS bunches)
Bunch length	560 ns
Injection duration	0.1 ms
Particles per pulse	$1.64 \cdot 10^{12}$

### HIGHER HARMONICS IN ACCELERATION VOLTAGES

The standard formula [5] for the synchrotron frequency in case of a pure sine-wave as acceleration region

$$f_s = f_{rev} \sqrt{-\frac{h\eta}{2\pi\beta_s^2 E_s} eV_{acc} \cos\phi_s} \quad (1)$$

gives 3332 Hz at RCS injection, where  $\phi_s=0$ . The ideas in [6] for dual harmonic signals,

$$V = V_1 \sin\phi + V_2 \sin(n\phi + \Phi_2)$$

$$\sin\phi_{s0} = \sin\phi_s + \frac{V_2}{V_1} \sin(n\phi_s + \Phi_2) \quad (2)$$

where  $V_1$  and  $V_2$  are amplitudes of main and higher harmonic,  $n$  the ratio of the harmonic numbers,  $\Phi_2$  the phase shift in rad at the higher frequency,  $\phi_{s0}$  the synchronous phase in case of a pure sine-wave, and  $\phi_s$  the

synchronous phase location at the fundamental with dual harmonics explain a modified synchrotron frequency:

$$\left( \frac{f_{s\_dual}}{f_{s\_pure}} \right)^2 = \frac{1}{\cos \phi_{s0}} \left[ \cos \phi_s + \frac{V_2}{V_1} n \cos(n\phi_s + \Phi_2) \right] \quad (3)$$

Equations (2) can be extended to multi-harmonics. As the RCS rf system operates at the fundamental ( $h=2$ ), it is sufficient to include only even harmonics. From cavity impedance in Fig. 1 and former measurements [7] it is reasonable to restrict the analysis to the harmonics ( $h=2, 4, 6, 8, \text{ and } 10$ ). The modified equations for RCS become:

$$\begin{aligned} \sin \phi_{s0} &= \sin \phi_s + \sum_{k=2}^5 \frac{V_{2k}}{V_2} \sin(k\phi_s + \Phi_{2k}) \\ \left( \frac{f_{s\_h2-10}}{f_{s\_h2}} \right)^2 &= \frac{\cos \phi_s}{\cos \phi_{s0}} + \sum_{k=2}^5 k \frac{V_{2k}}{V_2} \frac{\cos(k\phi_s + \Phi_{2k})}{\cos \phi_{s0}} \end{aligned} \quad (4)$$

A numerical solver computes  $\phi_s$  from  $\phi_{s0}$ , which is given at ( $h=2$ ).

### Setup and Consistency Check

With 11 cavities, and 5 harmonics in amplitude and phase, a careful bookkeeping is needed to keep the data consistent. We cannot sample all information in a single-shot, so we have to assume that machine and beam condition are quite stable from pulse to pulse. Also we have to identify, where an uncertainty is introduced into the set of signal transfer functions.

At the central gap of each cavity are a left and a right side capacitive divider, which connect to cables to the RCS LLRF control room. As shown in Fig. 3, the differential signals of each cavity are combined, and the CPL path of a directional coupler goes to a 4-channel sampling oscilloscope, which can store 5 million points for each channel and the output path goes to the digital LLRF system [8].

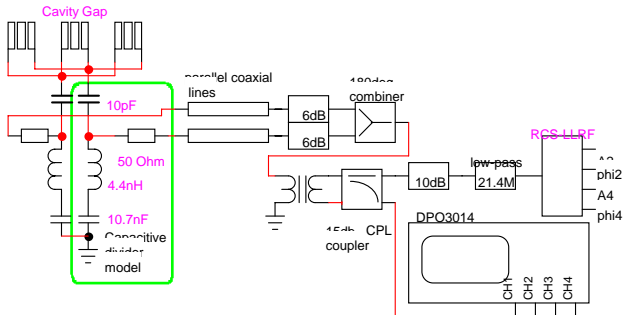


Figure 3: Simplified cavity gap signal path (only one system shown).

While the amplitudes  $A_2$  and  $A_4$  measured with the RCS LLRF system are consistent with the amplitudes of the harmonics ( $h=2$ ) and ( $h=4$ ) using the sampled oscilloscope data, earlier measurements using an older oscilloscope revealed that there is a phase difference due to the

### Radio Frequency Systems

#### T06 - Room Temperature RF

actual oscilloscope sample rate being different from the expected sample rate.

The cavity phase at ( $h=2$ ) is shown in Fig. 4 for cavity 2 with beam phase at cavity 3 without beam. With a linear offset, the phase is normalized to zero at beam injection and zero after beam extraction. The difference between both measurement methods (LLRF and scope) is in the order of  $0.6^\circ$  rms as shown in Fig. 5. The difference is modelled by a function  $k_{2/3}(f - f_0 + t \cdot k_t)$ , where  $f$  is the actual fundamental frequency,  $f_0=0.938175$  MHz is the frequency at injection,  $k_t=-35.78$  MHz/s is cavity independent, and  $k_2=2.5^\circ/\text{MHz}$  and  $k_3=3^\circ/\text{MHz}$  is individual for each system. If the oscilloscope clock is regarded as main error source, the error is equivalent to a 0.1 ppm offset of the 125 MHz sampling rate. However, different phase non-linearities in the two analogue signal paths from the 15 dB coupler to the AD-converters of either the LLRF-system or the scope may contribute, too.

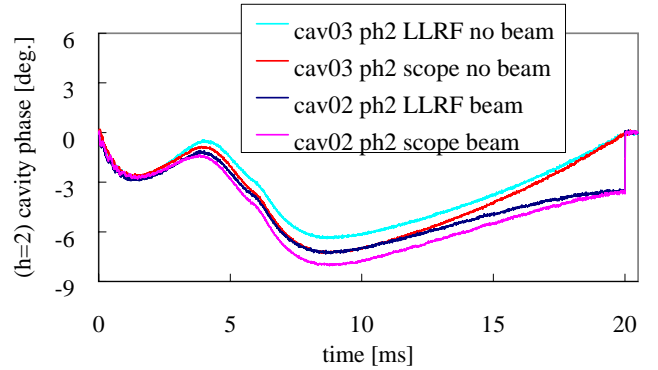


Figure 4: ( $h=2$ ) cavity phase: LLRF vs. scope data.

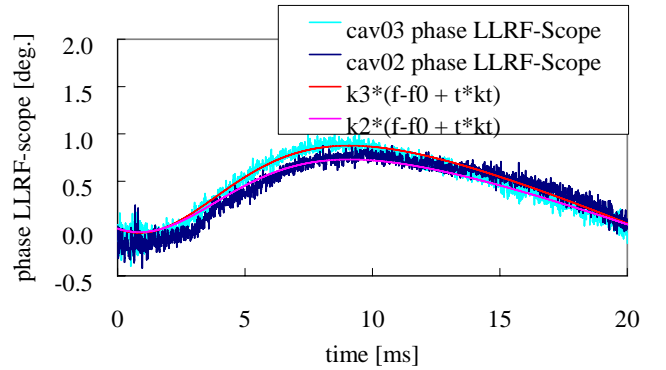


Figure 5: ( $h=2$ ) phase difference approximation.

### Evaluation of Multi-harmonic Data

The phase transfer function of the capacitive dividers (marked by a box in Fig. 3) as function of frequency has to be included to understand the phase relation between the harmonics. The circuit from Fig. 3 is modelled with  $<0.1^\circ$  error by the function:

$$\phi_{cap}(f) = 89.9^\circ - \arctan \frac{f / \text{MHz}}{0.15} \quad (5)$$

This formula means that the phase of the higher harmonic content of the rf voltage seen at the acceleration gap with such capacitance monitor differs from high-voltage probes measurements.

Taking into account that cavity 7 operated with 2 of 3 gaps, the vector sums relative to the fundamental ( $h=2$ ) of the harmonics  $h=4, 6, 8,$  and  $10$  are shown in Fig 6 (amplitude) and Fig. 7 (phase). The highest contribution is  $|h6|$ , and the lowest is  $|h8|$ . The harmonic content with beam in Fig. 8 shows -especially at  $|h4|$  - that the beam loading disappears, when the beam is extracted at 20 ms.

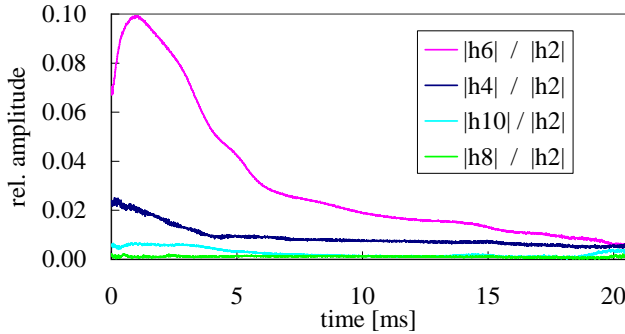


Figure 6: Relative higher harmonic content (no beam).

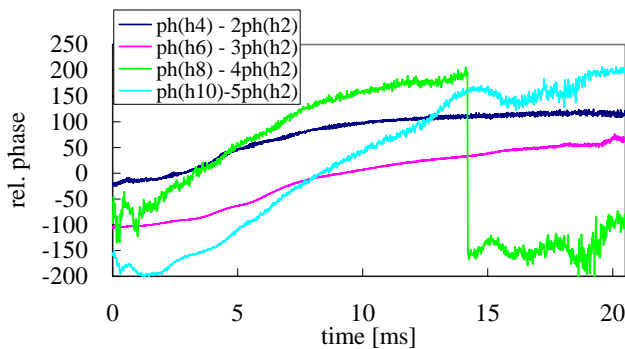


Figure 7: Relative phase of higher harmonics (no beam).

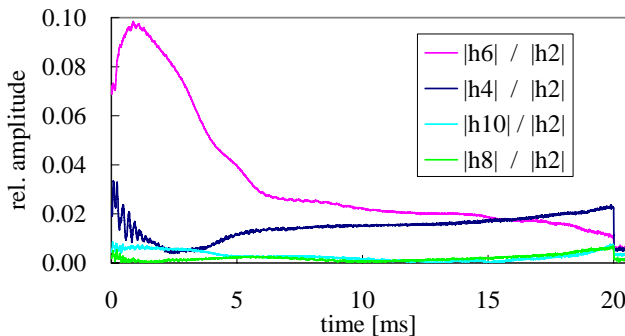


Figure 8: Relative higher harmonic content with beam.

The information from 5 vector-sums, collected from 11 cavities is inserted to eqn. (4). The standard synchronous phase  $\phi_{s0}$  at ( $h=2$ ) for a pure sine shown in dark blue in Fig. 9 is computed from energy-gain per turn and acceleration voltage scaled by 32/33 to model cavity 7 in 2 gap operation. A solver computes the phase  $\phi_s$  from  $\phi_{s0}$  for each  $10 \mu s$  time step. The calculated phase  $\phi_s$  with (green) and without beam (pink) is shown in Fig. 9, too. These curves are similar within  $<1^\circ$  after 0.5 ms, so the beam loading is still small. Assuming 25 mA Linac current at same bunch shape,  $\phi_s$  may vary by  $2 \dots 5^\circ$ . For comparison the measured phase difference between beam (by FCT) and cavity phase is plotted in light blue.

Although there is some phase ambiguity near injection, the higher harmonics can explain the measured synchronous phase deviation from eqn. (1). Fig. 10 shows the calculated effect of higher harmonics on the synchrotron frequency. Note, that in eqn. (4), the scaling factor for  $f_s^2$  is proportional to the harmonic number  $k$  times harmonic voltage. Depending on phase, same amplitude higher harmonics can have a bigger effect.

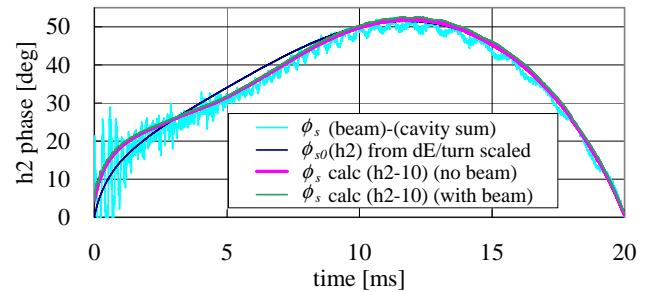


Figure 9: Measured and calculated synchronous phase.

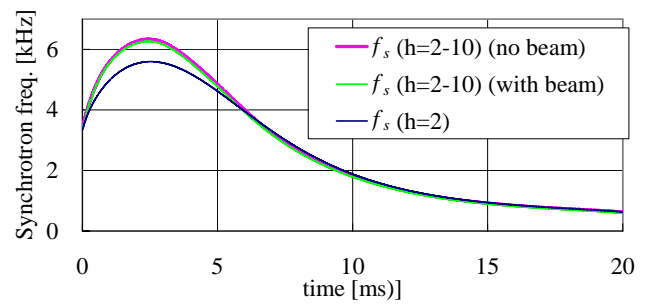


Figure 10: Calculated synchrotron frequency in RCS.

## SUMMARY

We show that effects of higher harmonics at broadband cavities can be modelled with multi-harmonic vector-sums related to the fundamental signals. This improves knowledge of the acceleration process and can help when we try beam loading compensation at higher intensity.

## REFERENCES

- [1] M. Kinsho, "J-PARC Progress and Challenges of Proton Synchrotrons", EPAC 2008, Italy, p. 2897.
- [2] M. Yoshii, et. al., "Present Status of J-PARC Ring RF systems", PAC2007, Albuquerque, USA, p. 1511.
- [3] M. Yoshii et. al., "The Status of the J-PARC RF Systems", EPAC 2008, Genoa, Italy, p. 285.
- [4] A. Schnase et. al. "MA cavities for J-PARC with controlled Q-value by external inductor", PAC2007, Albuquerque, New Mexico, USA, p. 2131.
- [5] Accelerator Physics and Engineering, 1998, ed. by A. Chao, M. Tigner (World Sci. Pub., Singapore), p.51.
- [6] E. Shaposhnikova et. al., "Study of Different Operating Modes of the 4<sup>th</sup> RF Harmonic Landau Damping System in CERN SPS", EPAC 1998, p. 978.
- [7] A. Schnase et. al., "J-PARC RCS Non-linear Frequency Sweep Analysis", EPAC 2008, p. 346.
- [8] F. Tamura, A. Schnase, and M. Yoshii, Phys. Rev. ST Accel. Beams 11, 072001 (2008).